

Multiple Surface Phase Shifting Interferometry

Leslie L. Deck*

Zygo Corporation

Laurel Brook Road, Middlefield, CT. 06455-0448

ABSTRACT

I show how phase shifting interferometry can be extended to account for multiple interference effects using a Fourier based analysis technique combined with wavelength tuning and a particular four-surface interferometer geometry. The technique is demonstrated by simultaneously measuring both surface profiles, the optical thickness variation and index homogeneity of a parallel plate. In addition, unlike traditional phase shifting techniques, the linear component of the homogeneity can be measured with high precision. It is shown that a significant linear component exists in a commercially supplied flat.

Keywords: Interferometry, phase shifting, metrology, homogeneity.

1. INTRODUCTION

Phase shifting interferometry¹ is the preferred technique for high-precision surface form measurements, but often performs poorly if the interferogram departs from strict 2-beam interference. This restriction has made it difficult to accurately profile transparent elements with parallel surfaces, parts that are of great interest to the optics, display and telecom industries. Most attempts to deal with multiple-surface interference have involved suppressing the unwanted surface reflections. Examples include applying index matching lacquers on the offending surface to reduce the reflected amplitude, broadband interferometry and grating interferometers to localize the interference at the surface of interest^{2,3}, grazing incidence interferometry to minimize the amount of energy transmitted to the unwanted surface⁴, and wavelength tuning with a PSI algorithm that specifically suppresses the interference frequencies from the unwanted surfaces⁵.

A different approach was proposed by Okada and Tsujiuchi⁶, who attempted to extract the information contained in the multi-beam interference pattern rather than suppress the unwanted interference. They realized that to first order, a multi-surface cavity is just a combinatorial collection of elemental 2-surface cavities, and that with wavelength tuning, each elemental cavity generates interference at a frequency directly related to the cavities' optical path difference (OPD). The Authors extracted the interferometric phases from all the elemental cavities by a least squares fit of the measured interferogram to a first-order approximation and demonstrated a 4-surface interferometer geometry that simultaneously measured the profiles of both surfaces of the plate and the index inhomogeneity.

The recent emergence of high quality wavelength-tunable sources for telecom applications makes wavelength tuning an even more attractive solution today. In this paper, I propose a new approach having a significantly greater flexibility and measurement precision than previous techniques. Rather than concentrating on a single surface or attempting to fit the interferogram to the 1st order frequencies through a least squares procedure, a complete Fourier analysis of the interference spectrum extracts the frequencies and phases of all the elemental cavities in a single wavelength-tuned measurement. The Fourier approach,

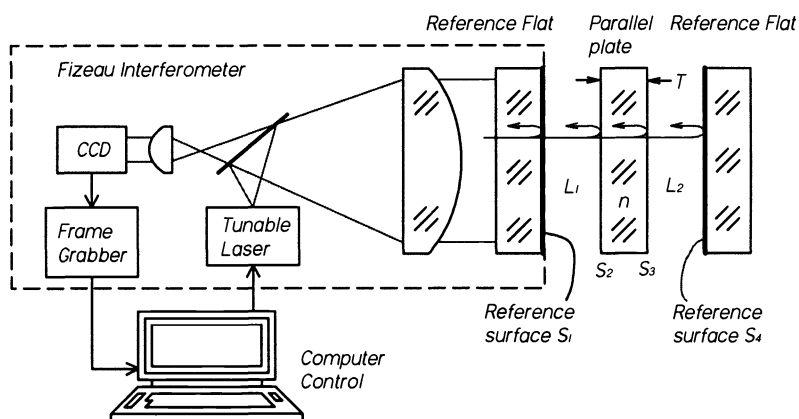


Figure 1: Apparatus used to demonstrate the method.

* email: ldeck@zygo.com

called Fourier transform phase-shifting interferometry (FTPSI)⁷, is highly robust and allows us to exploit the many mathematical tools developed for frequency-based analysis. The technique has wide applicability and is not limited to a particular measurement problem. An additional benefit from the ability to extract many surfaces from a single measurement means that the 3-dimensional relational characteristics between surfaces are preserved. It is therefore a logical replacement for PSI as a general-purpose approach to interferometric surface profiling.

The fundamentals of FTPSI are first explained and are applied to the measurement of a parallel plate. To fully exploit the capabilities of FTPSI, the interferometer geometry must isolate the 1st order frequencies of interest from the frequencies generated by other cavities. I therefore also describe a 4-surface interferometer geometry that isolates the 1st order frequencies from all frequencies out to 2nd order in surface reflectivity, producing simultaneous measurements of surface and optical thickness profiles with extremely high precision. The frequency isolation possible with this geometry, coupled with the relational information from FTPSI, produces high precision measurements of homogeneity that include the linear component – a term not measurable with traditional PSI methods. These capabilities are demonstrated with measurements of a commercially supplied parallel plate using a conventional Fizeau interferometer shown in Figure 1 outfitted with a wavelength tunable laser.

2. FOURIER TRANSFORM PHASE SHIFTING INTERFEROMETRY

Consider the interferogram produced by wavelength tuning in an elemental 2-surface interferometer cavity, such as the cavity formed between the two parallel surfaces S_1 and S_2 , denoted as $S_1:S_2$ in Figure 2. The surfaces are separated by a physical gap T containing a medium with refractive index n . The total phase difference φ between light rays with wavenumber k reflected from the first surface and light rays which reflect from the second surface p times is given by

$$\varphi(x, y) = 2pknT(x, y) + \Phi = 2pnT(x, y) \frac{2\pi\nu}{c} + \Phi, \quad (1)$$

where ν is the optical frequency of the light and Φ is an overall constant phase. The spatial variation of the phase is shown explicitly here but will be omitted in the equations that follow for the sake of clarity. Tuning the source optical frequency ν produces an interferometric phase variation $\dot{\varphi}$ that depends on the optical frequency tuning rate $\dot{\nu}$ and the cavity optical path difference $2pnT$ via

$$\dot{\varphi} = 4\pi pnT\dot{\nu}/c, \quad (2)$$

where the dot represents differentiation with respect to time. The cavity interference therefore varies at a frequency f_c ;

$$f_c = 2pnT\dot{\nu}/c. \quad (3)$$

Thus, in an elemental cavity, multiple reflection events produce interference at frequencies that are harmonics of the 1st order ($p = 1$) frequency.

The interferometric phase of any elemental cavity can be recovered from the complex amplitude of the Discrete Fourier Transform (DFT) of the interference, evaluated at the frequency f_c for that cavity:

$$\varphi = \tan^{-1} \left(\frac{\text{Im}(\text{DFT}(f_c))}{\text{Re}(\text{DFT}(f_c))} \right), \quad (4)$$

with

$$\text{DFT}(f_c) = \sum_{j=0}^{N-1} I_j W_j \exp(i2\pi j f_c / f_s) \quad (5)$$

and where the I_j represent the N intensity samples acquired during the wavelength tune, W_j are the sampling weights and f_s is the sampling rate. The reader should recognize the combination of Eqs. (4) and (5) as a formalized representation of traditional PSI algorithms. The optical frequency variation $\dot{\nu}$ is assumed linear throughout the acquisition.

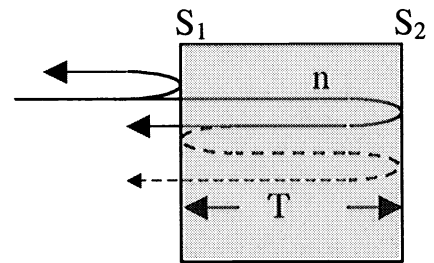


Figure 2: An elemental 2-surface cavity

The fidelity of the phase extraction depends on both the choice of Fourier window W and on how well the frequency of interest is isolated from other frequencies. The Hamming window was chosen in this analysis because it represents a good compromise between rapid spectral falloff and overall suppression. A good overview of the effect of window choice on the spectral response can be found in an article by Harris⁸. I now turn to the task of isolating the 1st order frequencies from themselves and higher order interference.

3. FOUR SURFACE CAVITY GEOMETRY

The 4-surface cavity of Figure 1 produces six elemental 2-surface cavities. The cavity bounded by surfaces S_2 and S_3 , denoted as $S_2:S_3$, is assumed to be a parallel plate of thickness T and index n , placed a distance L_1 from a reference surface S_1 . Another reference surface S_4 is placed a distance L_2 from S_3 . The values of the primary gaps L_1 and L_2 must be chosen so that all the elemental cavities have unique OPD's, and hence unique 1st order frequencies. However there are restrictions.

Recalling that the spectral resolution limit of a Fourier decomposition is inversely proportional to the observation time, the minimum resolvable interference frequency is

$$f_{\min} = \frac{1 + \mu}{\Delta t} = \frac{(1 + \mu)f_s}{N} \quad (6)$$

All 1st order frequencies must be separated by at least f_{\min} to be resolved. The parameter μ is introduced as a practical matter. The theoretical resolution limit occurs when $\mu = 0$, but in practice, the minimum resolvable frequency must be somewhat larger to account for instrumental deficiencies and phase error sensitivities. Eq. (3) with f_C equal to f_{\min} implies that the minimum resolvable OPD for a tuning range of $\Delta \nu_{\max}$ is

$$\Gamma = \frac{c(1 + \mu)}{\Delta \nu_{\max}} \quad (7)$$

This turns out to be about 3.75mm for an 80GHz maximum tuning range if $\mu = 0$. Clearly, the primary gaps must be greater than the limit imposed by Eq. (7).

The four surfaces produce six 1st order frequencies and twenty-seven 2nd order frequencies from 14 topologically distinct beam paths. Six of the twenty-seven 2nd order frequencies are identical to the 1st order frequencies and cannot be separated, but these contribute only an overall DC shift to the phase evaluation. The 1st order frequencies are not all independent, so it is not necessary to measure all six, however to be general, all six frequencies will be positioned to minimize the interference from neighboring 2nd order frequencies and each other. In terms of the primary gaps, the effective OPDs for the six 1st order cavities and the twenty-one different 2nd order cavities are given in the 2nd column of Table 1. The gaps given in Table 1 with Eq. (3) can be used to obtain the interference frequencies.

It is convenient to write the primary OPDs in terms of Γ .

Order	OPD	Frequency (f_C/f_{\min})
1 st	2nT	2
	2L ₁	2r
	2L ₂	2s
	2L ₁ +2nT	2+2r
	2nT+2L ₂	2+2s
	2L ₁ +2nT+2L ₂	2+2r+2s
2 nd	4L ₁	4r
	4nT	4
	4L ₂	4s
	4L ₁ +2nT	4r+2
	4L ₁ +2nT+2L ₂	4r+2+2s
	4L ₁ +4nT	4r+4
	4L ₁ +4nT+2L ₂	4r+4+2s
	2L ₁ +4nT	2r+4
	2L ₁ +4nT+2L ₂	2r+4+2s
	2L ₁ +2nT+4L ₂	2r+2+4s
	2L ₁ +4nT+4L ₂	2r+4+4s
	4nT+2L ₂	4+2s
	2nT+4L ₂	2+4s
	4nT+4L ₂	4+4s
	2L ₁ -2nT	2r-2
	2L ₁ +2L ₂	2r+2s
	2L ₁ -2nT-2L ₂	2-2r-2s
	2L ₁ -2L ₂	2r-2s
	2L ₁ +2nT-2L ₂	2+2r-2s
	2nT-2L ₂	2-2s
	4L ₁ +4nT+4L ₂	4r+4+4s

Table 1: The first six rows show the OPD and normalized frequency for the 1st order elementary cavities. The last 21 rows show the same data for the 21 unique 2nd order frequencies.

Define the number q as

$$q = nT/\Gamma, \quad (8)$$

the ratio of L_1 to nT as r ,

$$r = L_1/nT. \quad (9)$$

and the ratio of L_2 to nT as s ;

$$s = L_2/nT. \quad (10)$$

Column 3 of Table 1 shows the interference frequencies in terms of these variables normalized to f_{\min} . The frequencies scale with q , so the tuning range $\Delta\nu$ is adjusted to cancel this dependence

$$\Delta\nu = \Delta\nu_{\max}/q. \quad (11)$$

If nT is assumed to be the smallest optical gap, a search for values of r and s greater than one that maximizes the separation of the 2nd order from the 1st order frequencies reveals that $r = 3$, $s = 9$ is a good combination. In fact, a complete analysis shows that the optimal cavity geometry is one in which the ratio of the optical path lengths of any two primary gaps is a unique power of three.

With the tuning range and the gaps fixed, it remains only to determine the smallest number of samples N required. This is selected such that the largest 2nd order frequency (last row in Table 1) after being aliased to lower frequencies, is still greater than the largest 1st order frequency (6th row) by at least twice the spectral resolution limit. This constraint predicts

$$N = (1 + \mu)(6r + 8 + 6s), \quad (12)$$

which evaluates to 80 samples if $\mu = 0$.

Eqs. (11) and (12) with $r = 3$ and $s = 9$ together define the optimum cavity geometry and 1st order frequencies. Figure 3 shows the interference spectrum predicted for this configuration. The spectrum of 2nd order cavity frequencies is also shown to highlight the excellent separation between the 1st and 2nd order peaks.

The analysis methodology adopted can now be summarized; the interferometer cavity is constructed to create a unique OPD for each elemental cavity, thereby assuring unique interference frequencies. The interferogram is then sampled while the optical frequency is linearly chirped. The interferogram recorded at each pixel is spectrally decomposed with a Fourier transform and the interference frequency peaks corresponding to the elemental cavities are identified. Algorithms are then constructed for each of these frequencies using Eq. (5) and applied to the data to evaluate the phase of each elemental cavity separately.

4. SURFACE PROFILES AND OPTICAL THICKNESS

Associating each peak in Figure 3 with a particular elementary cavity is easy since the 1st order frequencies are set by the cavity geometry. The lowest frequency peak at $2f_{\min}$ (the first row in Table 1) is produced from the $S_2:S_3$ cavity. The spatial phase variation extracted at this frequency measures the optical thickness variation of the plate. The next higher peak at frequency $2rf_{\min}$ (the second row in Table 1) is produced from the $S_1:S_2$ cavity. Since the S_1 surface is assumed to be a well-characterized reference flat, the spatial phase variation from this frequency corresponds to the front surface profile of the plate. Finally, the spatial phase variation from the 4th peak at frequency $2sf_{\min}$ (the third row in Table 1) provides the back

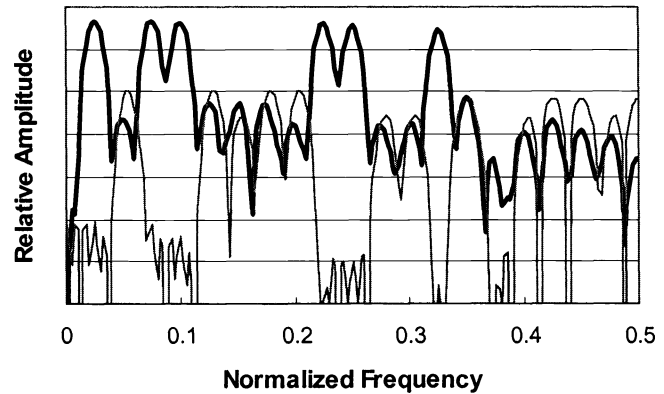


Figure 3: Log plot of the interference spectrum for the optimum 4-surface geometry normalized to the sampling rate. The heavy curve is the full spectrum and the light curve is the spectrum of 2nd order frequencies.

surface profile of the plate relative to reference flat S_4 . The back surface profile can be referenced to S_1 via a measurement of the $S_1:S_4$ cavity when the plate is removed, the so-called “empty cavity” measurement and subtracting this profile from the $S_3:S_4$ measurement. The empty cavity measurement is important for other measurement modes as well.

5. HOMOGENEITY

The relative index variation, or homogeneity, can be obtained with very high precision if nominal values for the index \bar{n} and plate thickness \bar{T} are supplied. Starting with the relations for the total phase observed at each primary cavity:

$$\varphi_{12} = 2kL_1, \quad (13)$$

$$\varphi_{23} = 2knT, \quad (14)$$

$$\varphi_{34} = 2kL_2 \quad (15)$$

where $k = 2\pi\nu/c$. A similar equation is found for the phase variation of the empty cavity

$$\varphi_{14} = 2k(L_1 + T + L_2). \quad (16)$$

Solving for the index n produces

$$n = \frac{\varphi_{23}}{\varphi_{14} - \varphi_{34} - \varphi_{12}}. \quad (17)$$

Since the phases φ represent total phases, not the modulo 2π phases obtained from the DFT, we can write for any cavity,

$$\varphi = 2k\bar{n}\bar{L} + \phi, \quad (18)$$

where \bar{n} and \bar{L} are nominal values of the index and gap, and ϕ is the local phase deviation from the total phase. Using this for each of the individual phases in Eq. (17) produces

$$n = \frac{2k\bar{n}\bar{T} + \phi_{23}}{2k\bar{T} + \phi_{14} - \phi_{34} - \phi_{12}}. \quad (19)$$

Noting that $2k\bar{T} \gg \phi_{14} - \phi_{34} - \phi_{12}$ for all plate thicknesses of interest, and keeping only terms to 1st order in $1/2k\bar{T}$, the index variation $\Delta n = n - \bar{n}$ is:

$$\Delta n = \frac{\phi_{23} - \bar{n}(\phi_{14} - \phi_{34} - \phi_{12})}{2k\bar{T}}. \quad (20)$$

The ϕ are determined from their respective unwrapped modulo- 2π phase maps, keeping in mind that ϕ_{14} is the phase map of the empty cavity.

It is important to note that in conventional homogeneity measurements, not only must the part be physically modified to eliminate multiple interference, but the spatial phase variation of each surface is obtained separately and their relative orientation is lost. Thus, *linear* variations in the homogeneity, often called homogeneity wedge, cannot be measured. Homogeneity wedge *can* be measured with FTPSI because the relative orientations of the spatial phase variations are preserved due to the simultaneous nature of the measurement. It is important to be able to measure these linear inhomogeneity components as they can adversely affect the performance of high quality lenses fabricated from the material.

The requirement of a time-separated empty cavity measurement is a potential weakness. Changes in the physical alignment of the two reference surfaces in the interval between the two measurements can lead to errors in the measured homogeneity. This potential problem can be greatly reduced if the parallel plate is smaller than the observable aperture because the area surrounding the plate can then serve as an indicator of cavity changes between the two measurements. If one assumes that only the S_4 surface can move as a rigid body, which is reasonable since the S_1 surface is typically connected to the instrument chassis, then any changes in the relative orientation of the S_4 surface can be measured and compensated for during the analysis.

6. MEASUREMENTS OF A PARALLEL PLATE

The methodology described above is demonstrated here by measuring a 30x50 mm, 8 mm thick fused silica glass plate with a nominal index of 1.457. The apparatus used is shown in Fig. 1 and consisted of a 100mm aperture Fizeau interferometer. The source was a 633nm tunable Vortex laser from New Focus with a maximum tuning range of 80GHz.

For $\mu = 0.5$, Eq. (8) produces $q=2.072$, implying $N=120$ frames from Eq. (12). Using Eqs. (9) and (10) the interferometer cavity was setup with nominally $L_1=34.97$ mm and $L_2=104.9$ mm. The actual surface positions were within 2mm of these nominal positions. Both S_1 and S_4 were high quality ($\lambda/20$) transmission and reference flats respectively. Figure 4 shows the static interference fringes observed on the interferometer monitor, the multiple interference fringes easily seen in the optic. The wavelength was tuned linearly over 38.6GHz (Eq. (11)) and 120 frames of 30Hz camera data were taken during the tune. Figure 5 shows that the frequency spectrum obtained from the intensity history of a typical pixel in the field is in excellent agreement with the theoretical spectrum shown in Fig. 3. All the 1st order frequencies were within 0.2 percent of the theoretically expected values, indicating that the interferometer cavity was constructed close to the desired geometry.

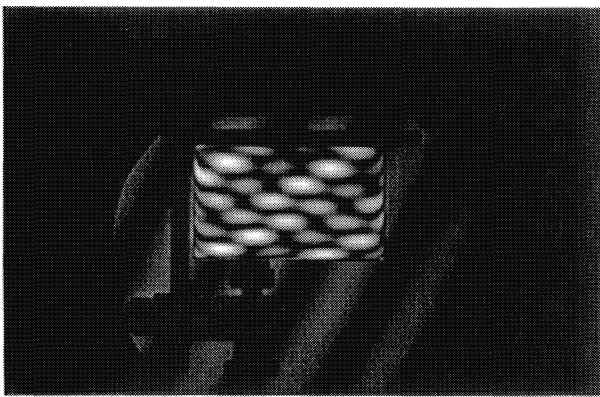


Figure 4: Interference observed from the four-surface cavity geometry. The (2-beam) interference between the two reference surfaces around the plate is also apparent.

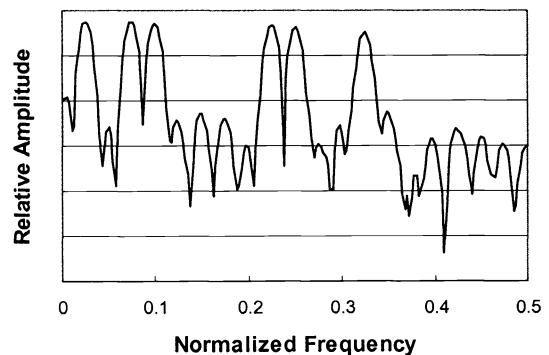


Figure 5: Log plot of the measured interference spectrum for the 4-surface geometry normalized to the sampling rate. The agreement with Fig. 3 is very good.

6.1. Surface profiles and optical thickness

Using the measured frequency of the 2nd and 4th interference peaks, the spatial phase variation of the 1st and 2nd surfaces of the flat (S_2 and S_3) were determined using Eqs. (4) and (5). Because the relative orientation is preserved in the measurement, the two surfaces can be represented as a 3-dimensional object. Figure 6 is a composite of the surface profiles relative to S_1 . The S_3 surface was referenced to the S_1 surface using the empty cavity measurement. Note however, the vertical scale perpendicular to the surfaces is different from the lateral scales to accentuate the surface features. To obtain the optical thickness profile, shown in Figure 7, the spatial phase variation of the lowest interference frequency as used.

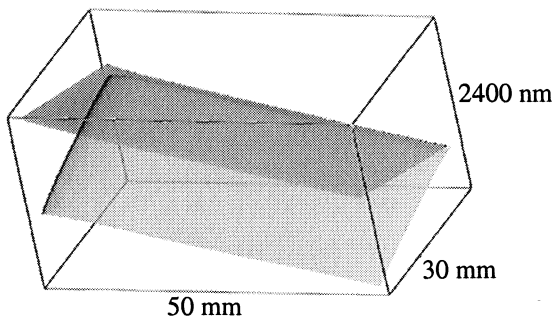


Figure 6: Composite of the profile measurements of the two surfaces of the 8mm parallel plate. Note the different scale of the vertical axis

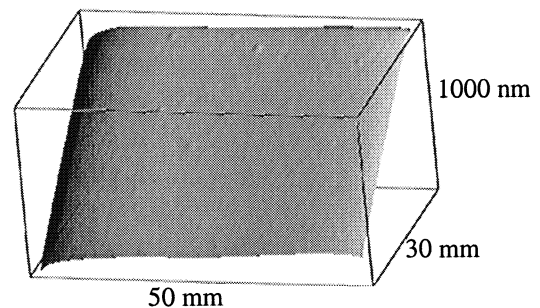


Figure 7: Optical thickness variation of the 8mm parallel plate. Note the different scale of the vertical axis

6.2. Homogeneity

The homogeneity measurement combines the spatial phase measurements ϕ_{23} , ϕ_{12} , ϕ_{34} of the three principle gaps with the phase measurement ϕ_{14} of the empty cavity and the nominal values of the index and thickness using Eq. (20). Figure 8 shows the homogeneity profile obtained from the 8mm parallel plate. A significant linear gradient of about $3\text{nm}/\text{mm}^2$ is observed along the long axis.

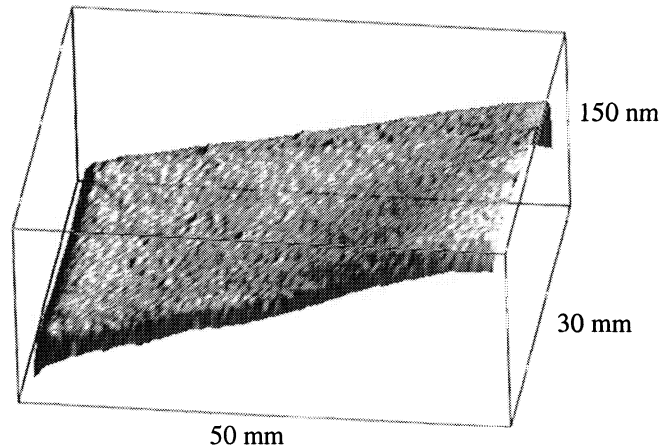


Figure 8: Homogeneity profile of the 8mm parallel plate. Note the different vertical axis scale

7. SUMMARY

This paper has outlined an effective, general methodology for treating multi-surface interferometric cavities so that reliable individual surface and optical thickness information can be obtained even in the presence of multiple reflection interference. The method uses wavelength tuning combined with a specific cavity geometry to eliminate multiple reflection interference out to second order and introduces a Fourier based analysis technique to optimally identify and extract the information for each desired surface. Measurements of an 8mm parallel plate demonstrated the technique by measuring both surfaces, the optical thickness and the index homogeneity. A notable feature of the technique is the ability to measure homogeneity wedge and it was determined that a significant homogeneity wedge existed in the parallel plate.

REFERENCES

-
- ¹ J. E. Greivenkamp and J. H. Bruning, "Phase Shifting Interferometry," *Optical Shop Testing*, D. Malacara, 501-598, J. Wiley, New York, 1992
 - ² K. Freischlad, "Large flat panel profiler", *Proc. Soc. Of Photo-Optical Inst. Eng.*, 2862, Flatness, Roughness and Discrete Defect Characterization for Computer Disks, Wafers and Flat Panel Displays. John C. Stover, Ed., 163-171, 1996
 - ³ P. de Groot, "Grating interferometer for flatness testing," *Opt. Lett.* **21(3)**, 228-230, 1996
 - ⁴ U.S. Pat. #5,923,425 to P. Dewa and A. Kulawiec
 - ⁵ P. de Groot, "Measurement of transparent plates with wavelength-tuned phase shifting interferometry", *Appl. Opt.* **39(16)**, 2658-2663, 2000
 - ⁶ K. Okada and J. Tsujiuchi, "Wavelength scanning interferometry for measurement of both surface shapes and refractive index inhomogeneity", *Proc. Soc. Of Photo-Optical Inst. Eng.*, 1162, Laser Interferometry: Quantitative analysis of interferograms, R.J.Pryputniewicz, Ed., 395-401, 1989

⁷ FTPSI is the topic of US and Foreign patents pending assigned to Zygo Corporation

⁸ F. J. Harris, "On the Use of Windows for Harmonic Analysis with the Discrete Fourier Transform," *Proc. IEEE*, **66(1)**, 51-83, 1978